A NEW SHAPE PRESERVING PARALLEL THINNING ALGORITHM FOR 3D DIGITAL IMAGES

P. K. SAHA, B. B. CHAUDHURI* and D. DUTTA MAJUMDER

Electronics and Communication Sciences Unit, Indian Statistical Institute, 203 Barrackpur Trunk Road, Calcutta 700035, India

(*Received* 25 *July* 1995; *in revised form* 30 *April* 1996)

Abstract—This paper is concerned with a new parallel thinning algorithm for three-dimensional digital images that preserves the topology and maintains their shape. We introduce an approach of selecting shape points and outer-layer used for erosion during each iteration. The approach produces good skeleton for different types of corners. The concept of using two image versions in thinning is introduced and its necessity in parallel thinning is justified. The robustness of the algorithm under pseudo-random noise as well as rotation with respect to shape properties is studied and the results are found to be satisfactory.

3D digital topology | Simple point | Outer-layer | Shape-point | Skeleton
Arc-skeleton | 3D parallel thinning | Sub-fields | Shape distance

1. INTRODUCTION

This paper is concerned with a new parallel thinning algorithm for three-dimensional (3D) digital images that preserves the topology and maintains their shape. 3D digital images are obtained by Computer Tomography (CT), Magnetic Resonance Imaging (MRI), Confocal Microscopy (CM), Ultrasound Echography (UE), Laser range Imaging (LRI) etc. The objective of 3D thinning is to produce a medial surface representation (sometimes a medial arc representation) that preserves the topology and maintains the shape of the object as much as possible.

Thinning is a powerful tool having application potentials in a wide variety of problems. It makes a compact representation of the objects that may be used for further processing. Thinning may be considered as a technique of data compression whereby the thinned representation and the thinning steps are stored, and the original image can be recovered by an inverse process. Thinning can be used in structural pattern matching and recognition problems. It is easy to segment structural features from the thinned version of the object. The presence of these features at particular relative positions is used for object recognition. These features may also be used to segment the object into meaningful parts. For example, Saha and Chaudhuri[1] proposed an efficient method to decompose an object from its thinned version.

Our long term goal is to find an efficient and robust algorithm for object recognition and description through thinning. In these tasks it is important to preserve the shape of the object in its thinned version. Otherwise, the features may not be proper representatives of the object.

Although thinning is an important tool for 3D image processing,[2,3] only a few publications[2–15] are available in the literature. Based on preservation of the Euler characteristic, Lobregt *et al.*[5] proposed an algorithm for detecting simple points that may be applied to 3D thinning. Unfortunately, their algorithm fails in some situations as pointed out in reference (9). Morgenthaler[16] described a parallel thinning algorithm based on his notion of "end" points which is different from the visible end points of curves or boundary points of surfaces. Based on path connectivity, Srihari *et al.*[2] described a sequential boundary removal algorithm for 3D thinning. Tsao and Fu[14] proposed a parallel 3D thinning algorithm based on the notion of surface connectivity. Hafford and Preston[4] extended the concept of sub-fields[16] in 3D and developed a parallel thinning algorithm for tetradecahedral tessellation. Mukherjee *et al.*[7] extended the 2D thinning algorithm SPTA[17] to develop a 3D thinning algorithm. In reference (18), Ma suggested sufficient conditions of 3D parallel reduction operator that preserves topology for (26, 6), (18, 6), (6, 26) and (6, 18) 3D digital images. In reference (3), Ma established the topological soundness of early results on parallel reduction operator[18] using the notion of minimal non-simple set. Many interesting properties of minimal non-simple set are also discussed.

All these papers stress on the preservations of topology in the thinned version. However, for shape preservation it is necessary but not sufficient to preserve only the topology of the object. "Shape" of an object is difficult to quantify. Gestalt psycho-physiologists proposed a large number of qualitative rules[19] to capture the notion of shape and form. Attneave[20] demonstrated that prominent information about object shape is concentrated at the boundary, especially at the corner of the object. It is also argued that shape is a property that is invariant under

* Author to whom correspondence should be addressed.

translation, rotation and scaling. However, a quantitative formulation of shape is yet to come.

In this paper we present a new parallel thinning algorithm for 3D objects so that its shape is maintained as much as possible. Since corner is an important shape attribute, behavior of this thinning algorithm around different types of corners is also studied. The notions of shape points and open points are introduced, and it is explained how these points are useful in global shape preservation. Robustness of the thinning algorithm under pseudo-random contour noise and rotation is studied and the results are presented.

A rigorous study on the detection of 3D simple points is presented in our previous publications.[8–10] However, the characterization of simple point along with other definitions and notations are presented in Section 2 for completeness and convenience of the readers. Theoretical aspects of the proposed thinning approach that produces a surface representation of 3D objects is described in Section 3. At the end of this section we provide a schematic description of the approach that produces an arc representation of an object from its surface representation. The parallel thinning algorithm is described and the experimental results are presented in Section 4. The robustness of the proposed algorithm under pseudo-random contour noise as well as rotation with respect to shape properties is studied and the results are described in Section 5.

2. GENERAL DEFINITIONS AND SIMPLE POINT CHARACTERIZATION

A 3D digital image is defined in a 3D array of lattice points represented by integer valued triples of Cartesian co ordinates (x, y, z). Let $p_1 = (x_1, y_1, z_1)$ and $p_2 = (x_2, y_2, z_2)$ be two points. The following definitions of adjacency relations[21] are used in this paper:

1. p_1, p_2 are *26-adjacent* if $\max\{|x_1 - x_2|, |y_1 - y_2|, |z_1 - z_2|\} \leq 1$.
2. p_1, p_2 are *18-adjacent* if $\max\{|x_1 - x_2|, |y_1 - y_2|, |z_1 - z_2|\} \leq 1$ and $|x_1 - x_2| + |y_1 - y_2| + |z_1 - z_2| < 2$.
3. p_1, p_2 are *6-adjacent* if $|x_1 - x_2| + |y_1 - y_2| + |z_1 - z_2| \leq 1$.

If p_1 is α-adjacent to p_2, where $\alpha \in \{6, 18, 26\}$, then p_1 is also called an *α-neighbor* of p_2.

Let S be a non-empty set of points. An *α-path* between two points p, q in S means a sequence of distinct points $p = p_0, p_1, \ldots, p_n = q$ in S such that p_i is α-adjacent to p_{i+1}, $0 \leq i < n$. An α-path is an *α-closed path* if p_0 is α-adjacent to p_n. Two points $p, q \in S$ are *α-connected* in S if there exists an α-path from p to q in S. An *α-component* of S is a maximal subset of S where each pair of points is α-connected. Let $p = (x_0, y_0, z_0)$ be a point. The *xy co-ordinate plane* through p is the set of all points $(x', y', z_0) | x', y'$ are integers. The yz and zx co-ordinate planes through p are defined similarly.

In the following discussions, $\mathcal{N}(p)$ is used to denote the set of 27 points in the $3 \times 3 \times 3$ neighborhood of p. Nomenclature of the points of $\mathcal{N}(p)$ is shown in Fig. 1. The set of points $\mathcal{N}(p) - \{p\}$ is denoted as $\mathcal{N}^*(p)$. We classify the points of $\mathcal{N}^*(p)$ according to their adjacency relations with p as follows:

s-point: An *s-point* is 6-adjacent to p.

e-point: An *e-point* is 18-adjacent but not 6-adjacent to p.

v-point: A *v-point* is 26-adjacent but not 18-adjacent to p.

Example. In Fig. 1, the points p_N, p_S, p_E, p_W, p_T, p_B are s-points of p; the points p_{TN}, p_{TS}, p_{TE}, p_{TW}, p_{BN}, p_{BS}, p_{BE}, p_{BW}, p_{NE}, p_{NW}, p_{SE}, p_{SW} are e-points of p while the points p_{TNE}, p_{TNW}, p_{TSE}, p_{TSW}, p_{BNE}, p_{BNW}, p_{BSE}, p_{BSW} are v-points of p.

Two s-points $a, b \in N(p)$ are called *opposite* if they are not 26-adjacent. Otherwise, they are called *non-opposite s-points*.

Example. In Fig. 1, the points p_N, p_S are opposite s-points while the points p_N, p_E are non-opposite s-points.

Let a, b, c denote three non-opposite s points of $\mathcal{N}(p)$. Then we define the following two functions:

- $e(a, b, p) = q | q \in \mathcal{N}^*(p)$ and 6-adjacent to a, b,
- $v(a, b, c, p) = q | q \in \mathcal{N}^*(p)$ and 6-adjacent to $e(a, b, p)$, $e(b, c, p)$, $e(c, a, p)$.

Example. If a, b, c denote the points p_N, p_T, p_E in $\mathcal{N}(p)$ then according to the above definitions $e(a, b, p)$ and $v(a, b, c, p)$ are denoted by the points p_{TN} and p_{TNE}, respectively. It may be noted that $e(a, b, p)$ is an e-point while $v(a, b, c, p)$ is a v point of $\mathcal{N}(p)$.

We define three more functions as follows:

- $f_1(a, p) = q | q \notin \mathcal{N}(p)$ and 6-adjacent to a,
- $f_2(a, b, p) = q$ $q \notin \mathcal{N}(p)$ and 6-adjacent to $f_1(a, p)$, $e(a, b, p)$,
- $f_3(a, b, p) = q | q \notin \mathcal{N}(p)$ and 6-adjacent to $f_2(a, b, p)$, $f_2(b, a, p)$.

Example. Let $p = (5, 5, 5)$ be a point while $a = (4, 5, 5)$ and $b = (5, 4, 5)$ be two non-opposite s-points of p. According to above definitions the point (3, 5, 5) represents $f_1(a, p)$ while the points (3, 4, 5) and (3, 3, 5) represent $f_2(a, b, p)$ and $f_3(a, b, p)$, respectively.

Let (a, d), (b, e), (c, f) denote three distinct unordered pairs of opposite s-points of $\mathcal{N}(p)$. Let condition C_1 be "$x \in \{b, e, c, f\}$": condition C_2 be "$x, y \in \{b, e, c, f\}$ and x, y are non-opposite"; condition C_3 be "$x \in \{b, e, c, f\}$ and $x \in \{p_N, p_S, p_W\}$"; condition C_4 be "$x, y \in \{b, e, c, f\}$; x, y are non-opposite and $x \in \{p_E, p_T, p_W\}$" and condition C_5 be "$x, y \in \{b, e, c, f\}$; x, y are non-opposite and $x, y \in \{p_E, p_S, p_W\}$".

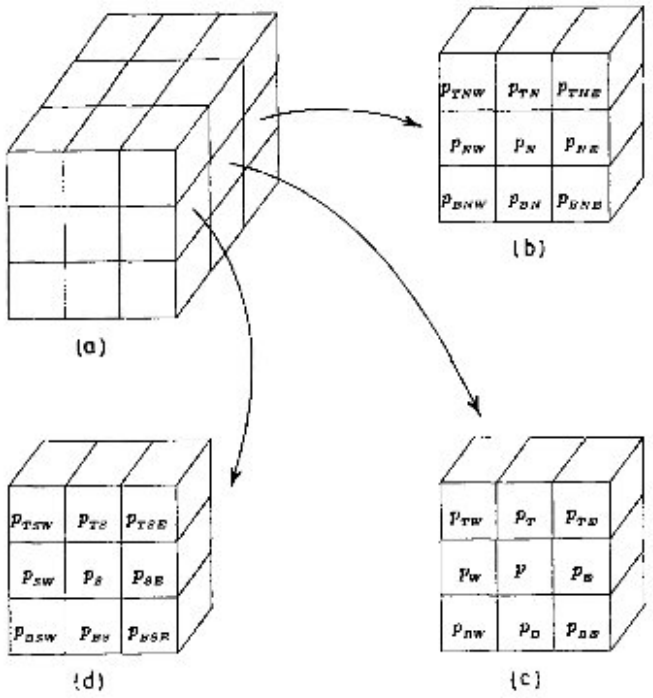

Fig. 1. Nomenclature of the points in the $3 \times 3 \times 3$ neighborhood of a point p. Clock-wise from top-left corner—neighborhood representation, black vertical plane, middle vertical plane, and front vertical plane.

We define a middle plane and an extended middle plane of $\mathcal{N}(p)$ as follows:

$$\mathcal{M}(a,d,p) = \{x|C_1\} \cup \{e(x,y,p)\ C_2\},$$
$$\mathcal{EM}(a,d,p) = \mathcal{M}(a,d,p) \cup \{f_1(x,p)|C_3\} \cup \{f_2(x,y,p)|C_4\} \cup \{f_3(x,y,p)|C_5\}.$$

We call $\mathcal{M}(a,d,p)$ and $\mathcal{EM}(a,d,p)$ as middle plane and extended middle plane of $\mathcal{N}(p)$, respectively.

Example. Considering a point $p = (5,5,5)$ and two of its opposite s-points $a = (4,5,5)$ and $d = (6,5,5)$ we have the middle plane $\mathcal{M}(a,d,p) = \{(5,5,4), (5,5,6), (5,4,5), (5,6,5), (5,4,4), (5,4,6), (5,6,4), (5,6,6)\}$ and the extended middle plane $\mathcal{EM}(a,d,p) = \{(5,5,4), (5,5,6), (5,4,5), (5,6,5), (5,4,4), (5,4,6), (5,6,4), (5,6,6), (5,5,3), (5,3,5), (5,4,3), (5,6,3), (5,3,4), (5,3,6), (5,3,3)\}$. It may be noted that $\mathcal{M}(a,d,p)$ contains eight points while $\mathcal{EM}(a,d,p)$ contains 15 points.

We also define a surface of $\mathcal{N}(p)$ as follows:

$$\text{surface}(a,p) = \{a\} \cup \{e(a,x,p)|C_1\} \cup \{v(a,x,y,p)|C_2\}.$$

Example. Considering $p = (5,5,5)$ and one its s-point $a = (4,5,5)$ we have surface$(a,p) = \{(4,5,5), (4,4,5), (4,6,5), (4,5,4), (4,5,6), (4,4,4), (4,4,6), (4,6,4), (4,6,6)\}$. It may be noted that surface(a,p) contains exactly nine points.

In this paper, we consider 26-adjacency for black points and 6-adjacency for white points. A 26-component of black points is a black component and a 6-component of white points is a white component. A simple characterization of (26, 6) simple points is established in our previous publications.[8–10] According to that characterization a point p is a (26, 6) simple point if and only if it satisfies the following four conditions:

1. p has at least one black 26-neighbor.
2. p has at least one white 6-neighbor.
3. The set of black 26-neighbors of p is 26 connected.
4. The set of white 6-neighbors of p is 6-connected in the set of white 18-neighbors of p.

In Section 3 we present the proposed new approach to 3D thinning algorithm. From now onward "simple point" will refer to "(26, 6) simple point" unless stated otherwise.

3. THE THINNING APPROACH

We initially consider thinning as an approach of producing a medial surface representation of a 3D digital object that preserves the topology and maintains the shape of the object as much as possible. It may be necessary in some applications to produce a medial arc representation of an object. We call this transformation process as arc-thinning and consider it at the end of this section. The proposed thinning approach producing a medial surface representation is an iterative erosion process that consists of two steps namely primary-thinning and final-thinning. The results of these steps are called primary skeleton and final skeleton, respectively.

Our thinning approach exploits the information from two versions of an image implicitly stored throughout the thinning procedure. One image version denotes the black/white configuration before the current iteration while the other denotes the current stage of the processed image. Here it is worthy to mention that simple points are always detected on the current version of the image while the shape preserving constraints are mostly defined on the image version before each current iteration. This idea is quite different from other researchers who used only one version of image for thinning.[4,15] In this context it is worthy to mention that only one image is physically stored throughout the thinning algorithm, although we refer to two image versions. Two image versions are realized from one physical image by the way of interpreting the values of image points which will be more clear from the subsequent discussion. At the beginning of the algorithm when we read an image, every white point is assigned a large negative number, say $-$maxint and each black point is assigned "0". At the beginning of execution all black points are unmarked. As the erosion continues, some of the black points are deleted and some are marked. Once a point is marked it is never deleted in subsequent steps of erosion during primary-thinning. Each iteration is denoted by an iteration number i. A threshold value thr is defined during ith iteration as follows:

$$\text{thr} = \text{maxint} + i.$$

If during ith iteration a point is found deletable then it is assigned the value thr. Thus, a point having value greater than or equal to thr is black before the iteration. Otherwise, the point is white before the iteration. A point with negative value is currently white, while a point with non-negative value is currently black. In this way, two image versions are realized from single physical image. A point with zero value is an unmarked black point. A point is marked by assigning the iteration number i. Thus, a point with non-zero positive value is a marked point.

At this point it should be made clear that in this paper "iteration" and "scan" are two completely different concepts. A "scan" is a traversal of the entire image through the thinning algorithm. On the other hand, an "iteration" is completed after considering the entire outer-layer of an object through proper topology and shape constraints. An iteration may consist of one or more scans. In case an iteration consists of more than one scan, the operation in each scan is generally different.

In an iterative erosion method of thinning, a 3D object is considered as an onion that consists of a finite number of layers. At each iteration we remove points from the outer-most layer in a topology and shape preserving manner. We call an outer-most layer as outer-layer. Outer-layer plays an important role in determining global shape of skeletons, especially, around the corners. Unfortunately, previous papers[2–7,12–15] did not make any extensive study on how the outer-layer could be defined to preserve the cornerity in the skeletons.

Before we describe our thinning procedure let us present some definitions and conditions in this context. In the following definitions and conditions (a,d), (b,e) and (c,f) denote three distinct unordered pairs of opposite s-points of $\mathcal{N}(p)$ unless stated otherwise.

Definition 1. During an iteration a black point p is an s-open point if at least one s-point of $\mathcal{N}(p)$ is white before the iteration.

Definition 2. During an iteration a black point p is an e-open point if p is not an s-open point and an e-point $e(a,b,p)$ is white while the points $f_1(a,p)$, $f_1(b,p)$ are black before the iteration.

Definition 3. During an iteration a black point p is a v-open point if p is neither an s-open point nor an e-open point and a v-point $v(a,b,c,p)$ is white while the points $f_1(a,p)$, $f_1(b,p)$, $f_1(c,p)$ are black before the iteration.

The set of s-open, e-open and v-open points define the outer-layer in an iteration. It is understood from the above definitions that the labeling of points as s-open, e-open and v-open points is made once before each iteration. In the definition of e-open points, the extra condition "$f_1(a,p)$, $f_1(b,p)$ are black" is used to include the point marked as "e" in Fig. 2 as an e-open point and at the same time to exclude the points marked as "$\times$" in Fig. 3 from e-open points. If the points marked as "$\times$" are included in e-open points i.e. considered for erosion in

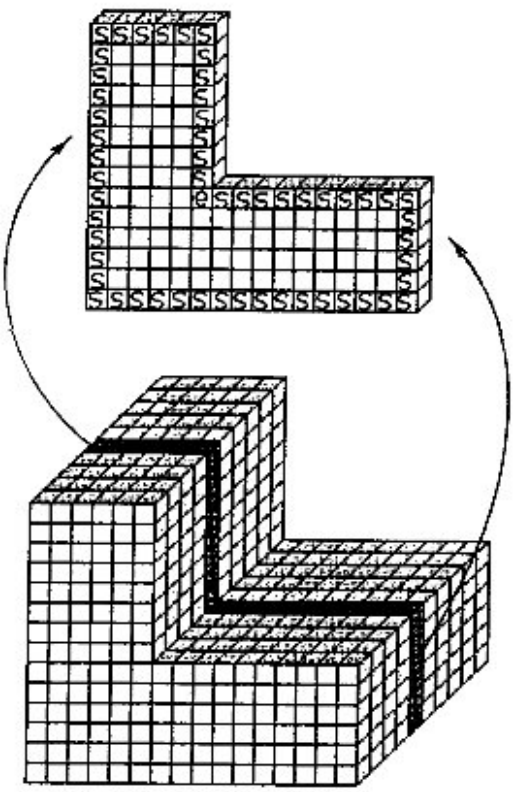

Fig. 2. Demonstration of e-open points. The point marked as "e" is an e-open point. Here, points marked as "s" are s-open points.

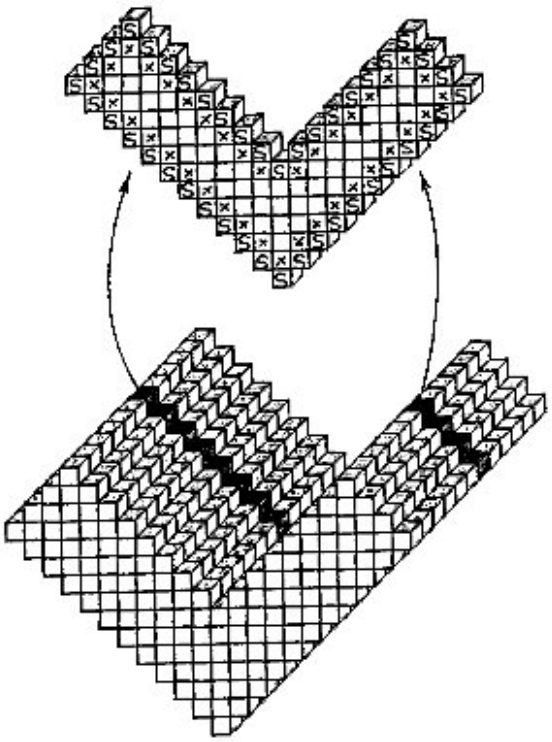

Fig. 3. The points marked as "×" are excluded from e-open points to preserve the sharpness of the corner. Here, points marked as "s" are s open points.

the particular iteration then the sharpness of the corner is lost in the next iteration. Similarly, the extra condition "$f_1(a,p)$, $f_1(b,p)$, $f_1(c,p)$ are black" is used in the definition of v-open points to preserve the sharpness at the corner where the three surfaces meet.

Condition 1. During an iteration a point p satisfies Condition 1 if there exist two opposite s-points $a, d \in \mathcal{N}(p)$ such that $\mathcal{EM}(a,d,p)$ contains a 6-closed path of white points encircling p and each of surface(a,p) and surface(d,p) contains at least one black point before the iteration.

A 6-closed path of $\mathcal{EM}(a,d,p)$ encircles p if it contains two points of $\mathcal{EM}(a,d,p) \cap \{p_T, p_N, p_E\}$. It is worthy to mention that in this paper a path or a closed path is a sequence of distinct points (see Section 2). It may also be noted that a 6-path of white points encircling p defines a tunnel[8–10,1,22] in the background. In the above condition for arc-like shape, the constraint that "$\mathcal{EM}(a,d,p)$ contains a 6-path of white points encircling p" characterizes an arc-like shape through p as shown in Fig. 4. In Fig. 4 the transparent voxels define a 6-closed path of white points in $\mathcal{EM}(a,d,p)$ encircling p. The constraint that surface(a,p) contains at least one black point characterizes that the arc-like shape has at least one point above $\mathcal{EM}(a,d,p)$. Similarly, the constraint that surface(d,p) contains at least one black point characterizes that the arc-like shape has at least one point below $\mathcal{EM}(a,d,p)$. Thus the second part of the condition

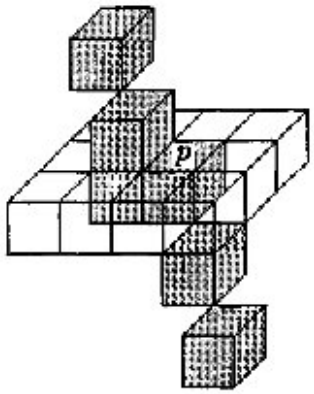

Fig. 4. Demonstration of arc-like shape. Transparent voxels define a 6-closed path of white points in $\mathcal{EM}(a,d,p)$. See text for details.

that "surface(a,p) and surface(d,p) contains at least one black point" ensures that the arc-like shape through p must be at least three points elongated. In other words, single point spikes or dents are never detected as arc-like shape.

Condition 2. During an iteration a point p satisfies Condition 2 if there exists a pair of opposite s-points (a,d) such that $d \in \{p_B, p_S, p_W\}$, a is white, d or $f_1(d,p)$ is white and each of the sets $\{e(a,b,p), b, e(b,d,p)\}$, $\{e(a,c,p), c, e(c,d,p)\}$, $\{e(a,e,p), e, e(d,e,p)\}$, $\{e(a,f,p), f, e(d,f,p)\}$, $\{v(a,b,c,p), e(b,c,p), v(b,c,d,p)\}$, $\{v(a,b,f,p), e(b,f,p), v(b,d,f,p)\}$, $\{v(a,c,e,p), e(c,e,p), v(c,d,e,p)\}$, $\{v(a,e,f,p), e(e,f,p), v(d,e,f,p)\}$ contains at least one black point before the iteration.

In the above condition for surface like shape, the constraint that "a is white, d or $f_1(d,p)$ is white" characterizes that p is a part of one or two points thick surface-like shape as shown in Fig. 5(a). To exclude a single point protrusions or dents from surface-like shape it is ensured that the surface-like shape through p [shown in Fig. 5(b)] has a minimum size of 3×3 points (including p). In other words, the projection of black points of $\mathcal{N}(p)$ along the a–d direction creates 3×3 points. Again, this is ensured by the constraint that each of the eight sets (mentioned in Condition 2) contains at least one black point. It may be noted that although 3×3 means nine points we need only eight sets (each set contributes one point in the projection) because p is always black. Thus, the second part of the condition for surface-like shape is used to exclude single point noise.

Definition 4. During an iteration a black point is a shape point if it satisfies Condition 1 or 2.

Thus, a shape point is either an arc-like shape or a surface-like shape. It may also be noted that shape points are labeled once before each iteration.

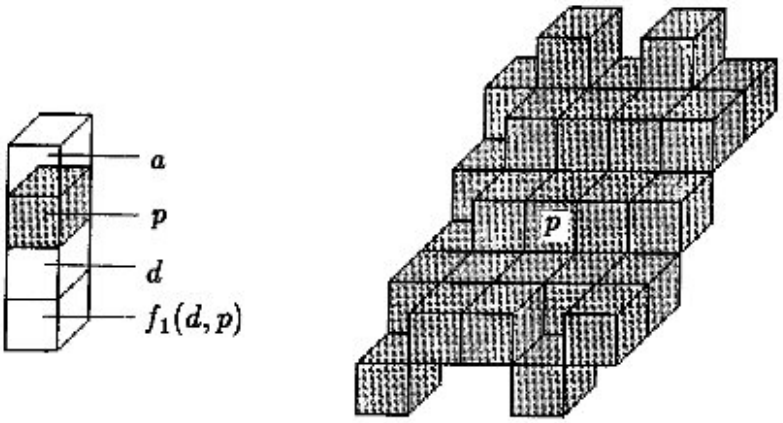

Fig. 5. Demonstration of surface-like shape. See text for details.

Condition 3. During an iteration a point p satisfies Condition 3 if each middle plane $\mathcal{M}(a,d,p)$ of $\mathcal{N}(p)$ holds that—either all e-points in $\mathcal{M}(a,d,p)$ are black before the iteration or the current black points of $\mathcal{M}(a,d,p)$ generate single 26-component without any tunnel.[10,11]

The black points of the middle plane $\mathcal{M}(a,d,p)$ generate a tunnel if and only if all the s-points of $\mathcal{N}(p)$ belonging to $\mathcal{M}(a,d,p)$ are currently black.

Definition 5. During an iteration a function is defined on the black/white configuration before the iteration as follows:

$$\text{thick}(a,d,p) = \begin{cases} 1 & \text{if } a, f_1(d,p) \text{ are white while } b,c,d \text{ are black,} \\ 0 & \text{otherwise.} \end{cases}$$

In the above definition "b,c,d are black" means that p has at least three black non-opposite s-points. In other words p has no two opposite s-points b, e such that both b and e are white before the iteration.

Condition 4. A point p satisfies Condition 4 if $\text{thick}(a,d,p)$, where $d \in \{p_B, p_S, p_W\}$, is true and the current black points of each of $\mathcal{M}(b,e,p)$ and $\mathcal{M}(c,f,p)$ generate single 26-component without any tunnel.

Condition 5. A point p satisfies Condition 5 if $\text{thick}(a,d,p)$, $\text{thick}(b,e,p)$, where $d,e \in \{p_B, p_S, p_W\}$, are true and the current black points of $\mathcal{M}(c,f,p)$ generate single 26-component without any tunnel.

Condition 6. A point p satisfies Condition 6 if $\text{thick}(a,d,p)$, $\text{thick}(b,e,p)$, and $\text{thick}(c,f,p)$, where $d,e,f \in \{p_B, p_S, p_W\}$, are true

Definition 6. During an iteration a black point is an erodable point if it is a simple point and satisfies any of the Conditions 4, 5 or 6.

3.1. Primary-thinning

As mentioned earlier primary-thinning is an iterative procedure and iterations are continued as long as any point is deleted in the last iteration. Each iteration is completed in three successive scans. During the first scan the set of unmarked s-open points is used for erosion. An unmarked s-open point is marked if it is a shape point. When it is not a shape point, it is deleted if it is a simple point, otherwise it is left unmarked. During the second scan the set of unmarked e-open points is used for erosion. It may be observed from Definitions 2 and 4 that an e-open point can never be a shape point and hence is never marked. However, an undesired situation may occur as shown in Fig. 6(c) when all unmarked e-open points satisfying the constraints of simple points[8–10] are deleted. It is worthy to illustrate this situation. Let us consider a 3D object shown in Fig. 6(a). During the first scan the set of s-open points are considered for erosion. Some of the s-open points are deleted while others are marked as shape points. The output after the first scan is shown in Fig. 6(b). In Fig. 6(b), some points are shown darker. It is interesting to note that the dark points of Fig. 6(b) are e-open points which are to be considered for erosion in the next scan of the same iteration. Let us consider that the direction of scanning along x-axis is from west to east. In that case the west-most e-open point becomes a simple point and gets deleted. After the west-most e-open point gets deleted the second west-most point becomes a simple point and gets deleted also. In this way all but the east-most e-open point gets deleted. This phenomenon creates an undesired drilling effect as shown in Fig. 6(c). It is interesting to note that deletion of e-open points as above does not change the topology of the 3D object. However, such drilling effects can be stopped if we impose 2D topology preservation in all co-ordinate planes (at most three) passing through the candidate e-open point and containing at least one white e-point before the iteration. It may be noted that Condition 3 basically checks 2D topology preservation in each co-ordinate plane passing through the candidate

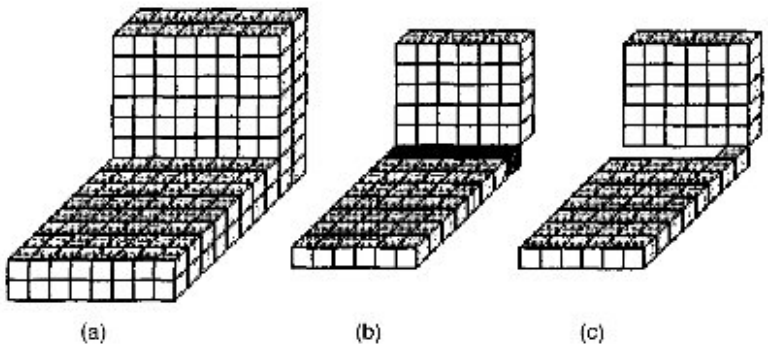

Fig. 6. Problem of eroding all simple e-open points. (a) Original object. (b) Set of points after the first scan. The points shown dark are e-open points. (c) Surface-skeleton when all simple e-open points are eroded.

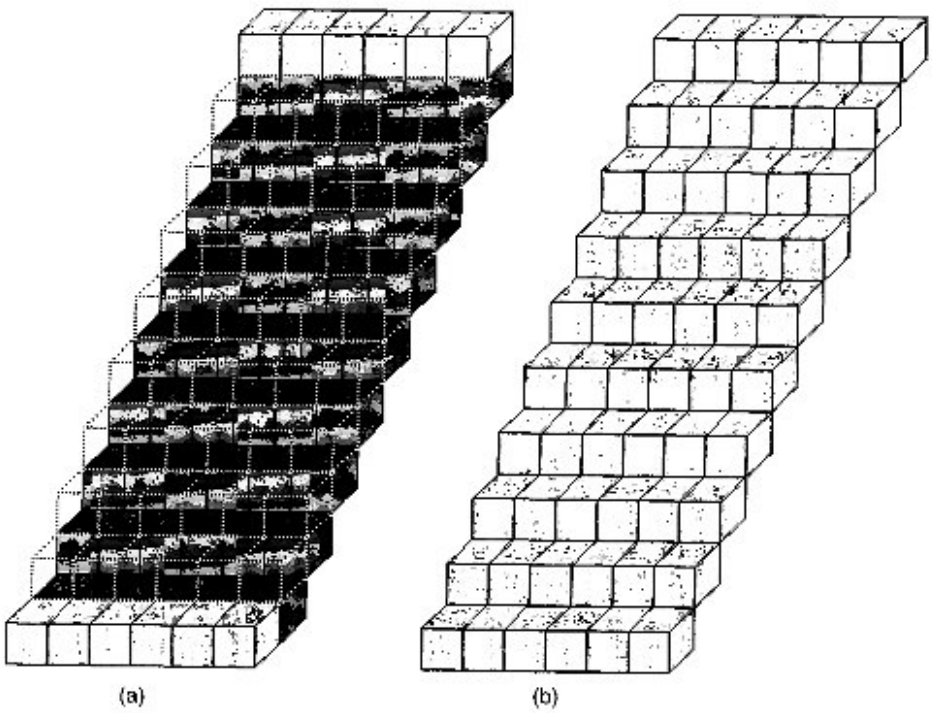

Fig. 7. (a) An output of primary-thinning. The transparent points sustain as surface-like shape across north-west direction while the dark points sustain as surface-like shape across the top-bottom direction. (b) Properly thinned output after final thinning.

point and containing one of its white (before the iteration) e-points. Thus, in the second scan an unmarked e-open point is deleted if it is a simple point and satisfies Condition 3. During the third scan the set of unmarked v-open points is used for erosion. An unmarked v-open point is deleted if it is a simple point.

3.2. *Final-thinning*

From the definition of shape point it may be understood that a two-point thick slanted surface may occur in the primary-skeleton. For example, a two-point thick slanted surface shown in Fig. 7(a) may result after primary thinning. The points shown by transparent voxels in Fig. 7(a) are obtained as surface-like shape across the top bottom direction while the points shown by dark voxels sustain as surface-like shape across the north-south direction. It may be noted that transparent points are thick points across the top-bottom direction while the dark points are thick points across the north-south direction. However, if we delete all thick points satisfying the constraint of simple point, undesired situation may occur. For example, the entire two points thick surface of Fig. 7(a) will be reduced to three connected lines. To overcome such problems an additional constraint of 2D topology preservation in the co-ordinate planes passing through the candidate point is subjected to the deletion of thick points. Such deletable thick points are called erodable points (see Definition 6). The procedure that removes undesired thick points and produces the proper

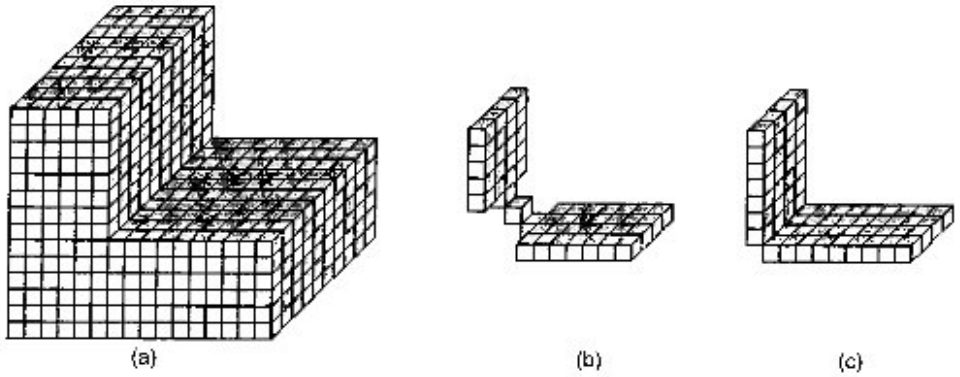

Fig. 8. Problem of considering 6-contour points for erosion during each iteration. (a) Original object. (b) Skeleton using 6-contour points. (c) Skeleton using s-open, e-open and v-open points separately for erosion.

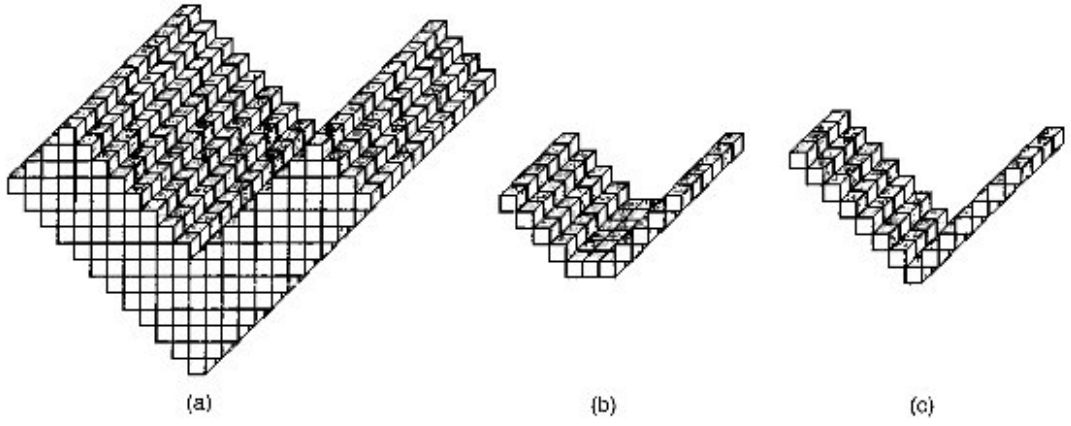

Fig. 9. Problem of considering 26-contour points for erosion during each iteration. (a) Original object. (b) Skeleton using 26-contour points. (c) Skeleton using s-open, e-open and v-open points separately for erosion.

skeleton from a primary skeleton is called final thinning. This is a single iteration procedure and the iteration consists of single scan. During this scan a black point p (irrespective of whether p is marked or unmarked) is deleted if it is an erodable point. The output of final thinning for corresponding pattern of Fig. 7(a) is shown in Fig. 7(b) which is properly thinned. Also, final thinning produces similar thinned output for two-point thick slanted surfaces [like Fig. 7(a)] in different directions.

3.3. Shape preservation around corners

Intuitively, it is obvious that the quality of skeleton gets affected by the sequence in which the points are deleted when outer-layer is defined on the current version of the processed image. This problem does not occur when the image before each current iteration is considered to label the outer-layer. It is already mentioned that in the proposed algorithm the outer-layer, i.e. the set of different open points are labeled before each current iteration. Even if the outer-layer is labeled before each current iteration, it may behave improperly around different corners. For example, if the set of 6-contour points (a black point having a white 6-neighbor before the current iteration is a 6-contour point) is used as outer layer then an undesired situation may arise as shown in Fig. 8. On the other hand, if the set of 26-contour points (a black point having a white 26-neighbor before the current iteration is a 26-contour point) is used as outer-layer then it produces a proper skeleton for the object of Fig. 8(a) but fails to produce a desired skeleton for the object of Fig. 9(a) [see Fig. 9(b)]. The approach of using s-open points, e-open points and v-open points for erosion during each iteration in three successive scans as described in Section 3.1, produces proper skeletons for both the objects as shown in Fig. 8(c) and Fig. 9(c). Here, proper skeleton means that the sharpness of meeting corners of two or more surfaces are preserved. Our approach is applied on different other types of corners with different angles and rotations and the skeletons are found quite satisfactory. A quantitative study on the behavior of the algorithm under rotation is demonstrated in Section 5.2.

3.4. Contour noise handling

Since noise is a part of real life, a good thinning algorithm should be robust enough to preserve the shape

of skeleton under noise. Unfortunately, it is not easy to distinguish the noise from an image. We consider a model of noise which consists of adding simple points of the background to the object, or deleting simple points from the object. The probability to change the type of a point is the measure of the noise. Thus, single point protrusions or dents on the contour are created as noise in the proposed model and we ensure that they do not produce undesired skeletal parts or branches. The definition of shape point serves the purpose. Branches are allowed to grow only from the shape points. Conditions 1 and 2 for shape points stop the creation of undesired branches from single point protrusions or dents. Our technique of contour noise handling is supported by experimental results shown in Figs 10–13. Also, a quantitative study on the behavior of the algorithm under pseudo-random contour

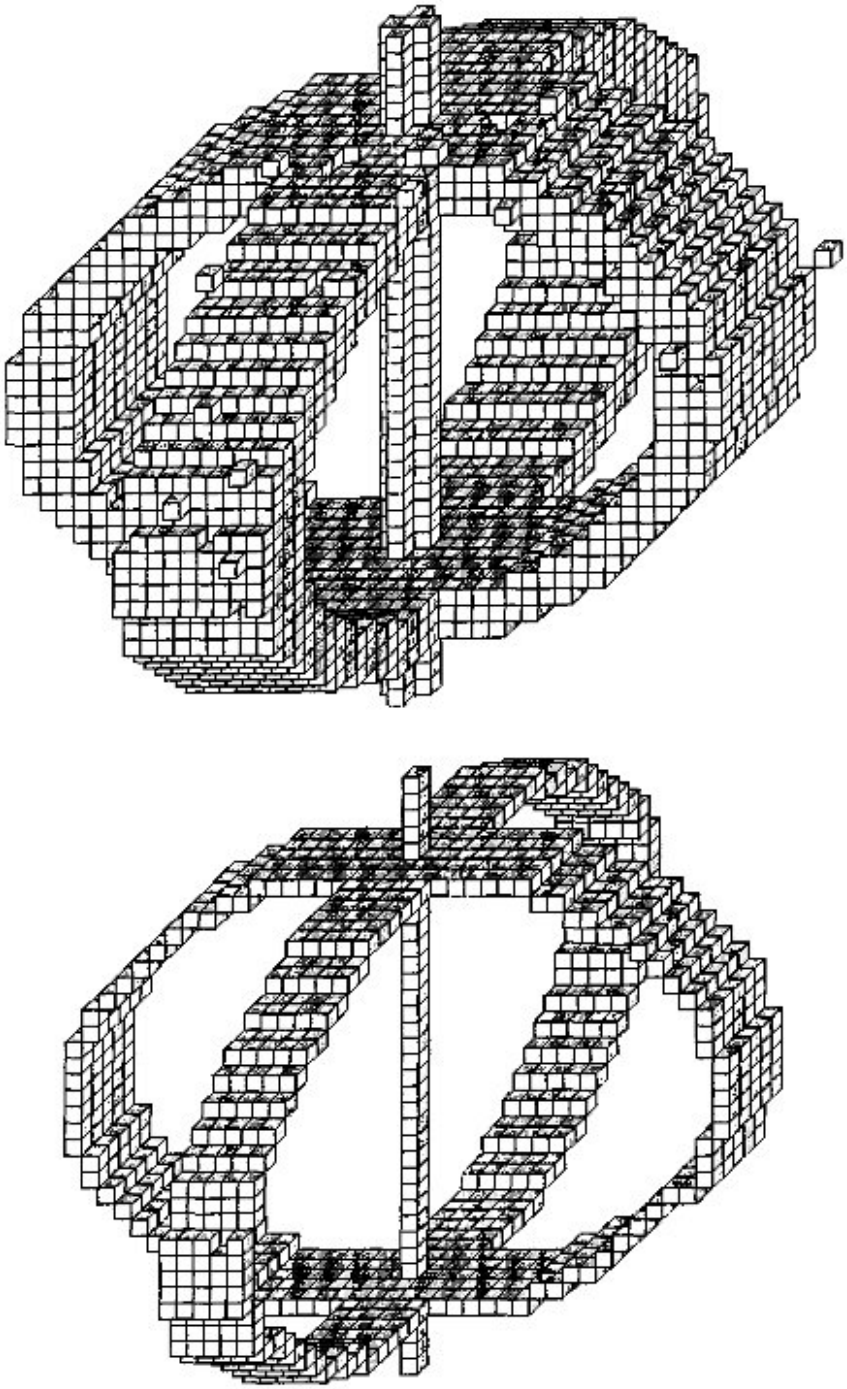

Fig. 10. Results of thinning. (a) Original object. (b) Skeleton. (c) Arc-skeleton.

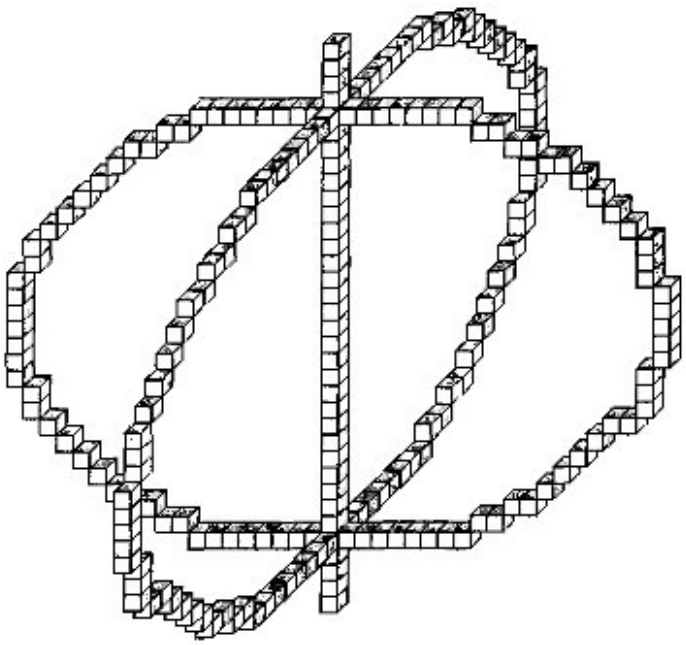

Fig. 10. (Continued).

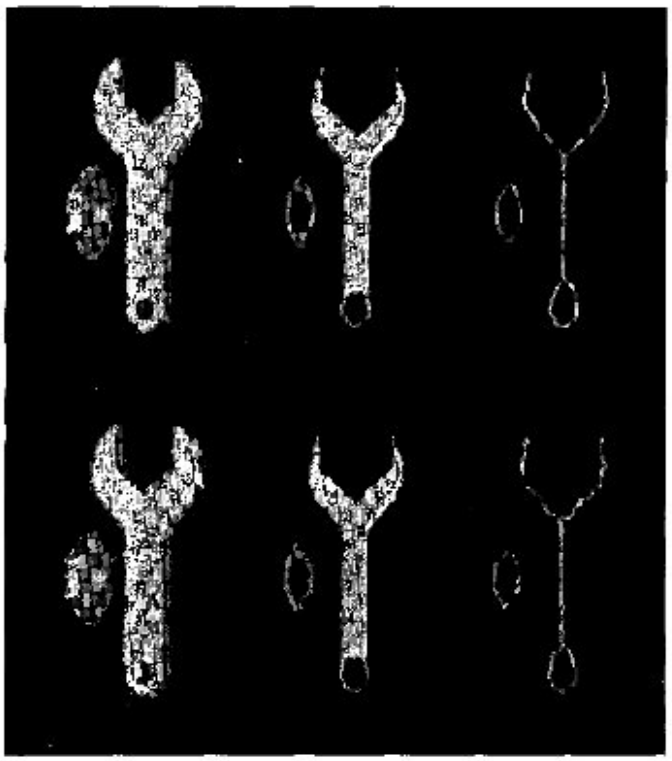

Fig. 11. Results of thinning. Top row (from left to right): original object, skeleton and arc-skeleton. Bottom row (from left to right): original object with noise, skeleton and arc-skeleton.

noise is demonstrated in Section 5.1. It is true that random noise does not produce only simple points and more involved distortion in shape is possible. But it becomes difficult to recognize and take care of non-simple noise points. However, if the noise energy is small, it is likely that most noise points are simple points when our approach will be very effective and useful.

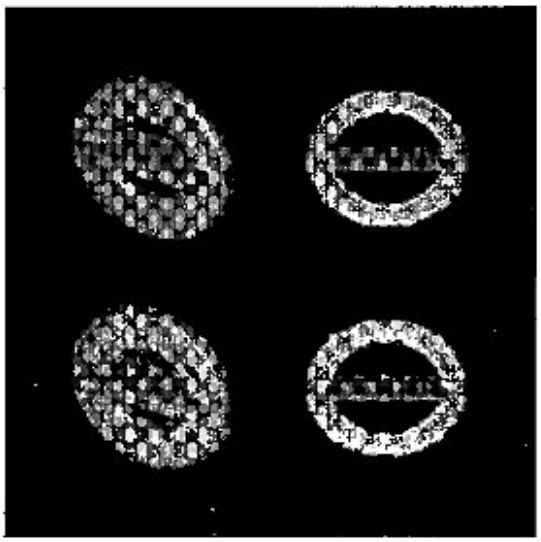

Fig. 12. Results of thinning. Top row (from left to right): original object and skeleton. Bottom row (from left to right): original object with noise and skeleton (here, objects and skeletons are shown from different angle to produce a better view).

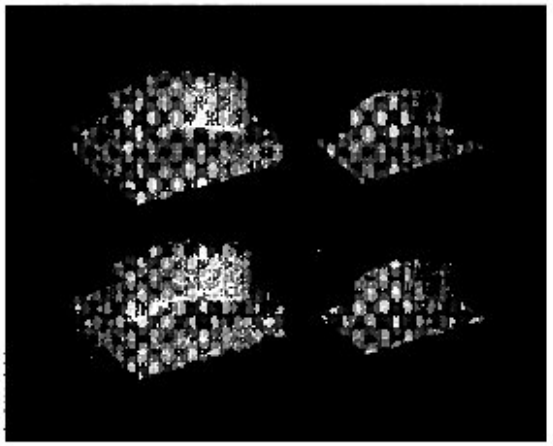

Fig. 13. Results of thinning. Top row (from left to right): original object and skeleton. Bottom row (from left to right): original object with noise and skeleton.

3.5. *ARC thinning*

Depending on the applications we sometimes need arc representation of an object. Here we present a schematic description of the procedure that produces a medial arc representation of an object from its surface representation. To avoid ambiguity we call this procedure as arc-thinning. Arc-thinning is also an iterative procedure with two steps, namely primary-arc-thinning and final-arc-thinning. The results of these steps are called primary-arc-skeleton and final-arc-skeleton, respectively. Here too we memorize two image versions in the same way described earlier. At first we put some definitions in this context. In the following definitions (a,d), (b,e) and (c,f) denote three distinct unordered pairs of opposite s-points of $\mathcal{N}(p)$.

Definition 7. During an iteration a black point p is an s-open-surface point if the points a, $e(a,b,p)$, b, $e(b,d,p)$, d are all white before the iteration.

Definition 8. During an iteration a point p is an e-open-surface point if it is not an s-open-surface point and at least one point from each sets $\{a\}$, $\{e(a,b,p), e(a,c,p)\}$, $\{v(a,b,c,p)\}$, $\{e(b,c,p)\}$, $\{v(b,c,d,p)\}$, $\{e(b,d,p), e(c,d,p)\}$, $\{d\}$ is while while each of the sets $\{f_2(a,b,p), f_3(a,b,p), f_2(b,a,p), f_1(b,p), f_2(b,d,p), f_3(b,d,p), f_2(d,b,p)\}$ and $\{f_2(a,c,p), f_3(a,c,p), f_2(c,a,p), f_1(c,p), f_2(c,d,p), f_3(c,d,p), f_2(d,c,p)\}$ contains at least one black point before the iteration.

During arc-thinning, the set of s- and e-open-surface points defines the outer-layer and they are labeled once

before each iteration. It may be noted from the above definitions that in an s-open surface point there is a 6-path of white points between two opposite s-points through another s-point and in case of e open surface points there is a 6-path of white points between two opposite s-points through an e-point. In case of e-open-surface points the second part of the condition is imposed to preserve the sharpness of corners during thinning (similar to the reasons explained for Definitions 2 and 3).

Definition 9. A black point is an arc-shape point if it satisfies Condition 1.

Thus, an arc-shape point is an arc-like shape which is at least three points elongated. Similar to shape points arc-shape points are also labeled once before each iteration.

Definition 10. A black point p is an arc-erodable point if: (i) every middle plane of $\mathcal{N}(p)$ contains at least one currently black point, and (ii) p is a simple point.

At the beginning of arc-thinning all black points are unmarked black points. As the erosion continues some of the black points are deleted and some are marked. Each iteration is completed in two scans. During the first scan an unmarked s-open-surface point p is marked if it is an arc-shape point. Otherwise, if p is a simple point then it is deleted else it is left unmarked. During the second scan an unmarked e-open-surface point is deleted if it is a simple point. Otherwise, the point is left unmarked. Final arc-thinning is a single scan procedure. During this scan a black point p (irrespective of whether it is marked or not) is deleted if p is an arc-erodable point.

4. THE PARALLEL THINNING APPROACH

In this section we describe a parallel thinning algorithm based on the approach discussed in Section 3. As discussed there, some shape and topology constraints are checked to mark or to delete a point. The most important problem faced by a parallel thinning algorithm is that two points p,q individually satisfy the necessary topology constraints for deletion but if both of them are deleted together then the topology constraints may be violated.[14] This condition may occur only when p,q are 26-adjacent. This is because the topology constraints for a point p are defined in its 26-neighborhood $\mathcal{N}(p)$ only. So, if two points p,q are not 26 adjacent then $\mathcal{N}(p) \cap q = \phi$, $\mathcal{N}(q) \cap p = \phi$, and obviously $p \cap q = \phi$. To solve this problem we use the concept of sub-fields.[4,16] An image is partitioned into eight disjoint subsets such that no two members p,q in the same subset are 26-adjacent. Hence, the members of each subset may be used for parallel erosion. Eight subsets $O_0, O_1, \ldots, O_7$ are defined as follows:

$$O_l = \{(2 \times i + f, 2 \times j - g, 2 \times k + h) \mid i,j,k = 0, \pm 1, +2, \ldots; f,g,h \in \{0,1\} \text{ and } 2^2 \times f + 2^1 \times g + 2^0 \times h = l\}. \quad (1)$$

such that two points $p,q \in O_l$ are never 26-adjacent. Each scan of the thinning algorithm may be completed in eight cycles and at lth cycle the image subset O_l is subjected to parallel erosion. The parallel algorithm requires $m^3/8$ processors for an image of size $m \times m \times m$ and it needs 8 cycles to complete each scan. Here, image size means the size of the smallest rectangular parallelepiped that encloses the set of black points. It is also possible to implement the algorithm with $m^3/8n$ processors for an integer n and in that case each scan requires $8n$ cycles instead of 8. The concept of sub-fields in two-dimensional hexagonal tessellation was earlier proposed by Golay[16] where he used three sub-fields to carry out one scan of topology preserving skeletonization. This concept was further studied by Hafford and Preston[4] in three-dimensional tetradecahedral tessellation. They used six sub-fields to carry out one scan of topology preserving skeletonization. While they stress on topology preservation and use only one version of image for thinning, we use two versions of image that makes a lot of improvements in maintaining the shape of skeletons. In Section 4.1 we have justified the utilization of two image versions in producing a better shape in the skeleton.

To test the effectiveness of the proposed algorithm it is applied on synthetically generated 3D objects as shown in Figs 10,11,12 and 13. In Figs 11,12 and 13 the background is made dark to render a better visual effect. The 3D objects in Figs 10,11,12 and 13 may be enclosed in minimum rectangular space of size $44 \times 41 \times 44$, $63 \times 136 \times 35$, $79 \times 79 \times 31$ and $81 \times 42 \times 62$, respectively. Fig. 10 contains typical additive and subtractive noises. Figs 11,12 and 13 have both noiseless and noisy versions. The noise in Figs 11,12 and 13 is generated in a pseudo-random manner while the noise in Fig. 10 is imparted manually to incorporate all typical possibilities. Arc-thinning is considered on Figs 10 and 11 only (meaningful result cannot be obtained by arc-thinning for Figs 12 and 13). In Fig. 10 the thinned surface and arc representations show the desirable shape despite noise. The surface and arc representations of both noiseless and noisy versions in Fig. 11 as well as the surface representations in Figs 12 and 13 are visually satisfactory.

4.1. *Utility of two image versions*

Consider the ith cycle of certain iteration in which the image subset O_i is used for erosion. During the erosion of ith cycle some of the points of O_i will be deleted. Since the points of O_i are not 26-adjacent, some undesired local spikes may be created in the current image. Now, if the shape constraints are defined on the current image while eroding the points of O_{i+1} in the next cycle then undesired branches may occur from the local spikes created in the current image version. This fact suggests that a prior version of the image should be memorized to define the shape constraints. It may be interesting to note that different open points, shape points are labeled before each current iteration in the proposed thinning approach

and as a result of this the local spikes in the current image do not affect the skeleton.

5. SHAPE ANALYSIS UNDER NOISE AND ROTATION

To study the behavior of the proposed algorithm under noise and rotation we define a shape distance function for 3D digital objects that will be useful in this context. A shape distance metric for 3D objects in E^3 was proposed by Banerjee *et. al.*[23] and Dutta Majumder.[24] They considered a subset A in E^3 as an object if: (1) A is compact, (2) Interior(A) is non-empty and connected, and (3) Closure(Interior(A))$=A$. The shape distance is defined as follows: let C be the class of all objects in E^3 which have the center of gravity at the origin $(0,0,0)$ and have unit volume. Any rotation of an object in E^3 about the origin $(0,0,0)$ is determined by the corresponding rotation of the system of axes which is, in turn, specified by three angles θ, ω and ψ in $[0°, 360°]$ where θ is the angle between the new and the old x-axis, ω is the angle between the new and the old y-axis and ψ is the angle between the new and the old z-axis. Let $A_{\theta,\omega,\psi}$ denote the rotated form of an object A in C, where θ, ω and ψ determine the new system of axes. It is clear that $A_{\theta,\omega,\psi}$ is in C. Rotation defines an equivalence relation on C. This equivalence relation is denoted by $\mathscr{R}$. The shape of an object is defined as an equivalence class generated by $\mathscr{R}$ in C. Let τ be the family of all such equivalence classes, i.e. of all shapes. D_1 is a distance function on C such that for $A, B \in C$,

$$D_1(A,B) = \text{Leb}_3((A-B) \cup (B-A)),$$

where Leb_3 is the Lebesgue measure in E^3. As shown in reference (23), D_1 defines a metric on C. D_2 is a distance function on C such that for $A, B \subset C$.

$$D_2(A,B) = \min_{\theta,\omega,\psi} D_1(A, B_{\theta,\omega,\psi}),$$

D_2 is a metric on τ.

Here, we propose a modified shape distance function between two objects in a 3D digital space that may be useful for estimation of shape distortion in thinning under noise and rotation. According to our requirement we restrict ourselves to the assumption that the distance function is applied on the objects with normalized size and rotation.

Definition 11. DT_1 is a distance function between two points $p_1=(x_1,y_1,z_1)$ and $p_2=(x_2,y_2,z_2)$ defined as follows:

$$\text{DT}_1(p_1,p_2) = \sqrt{(x_1-x_2)^2+(y_1-y_2)^2+(z_1-z_2)^2},$$

DT_1 is the Euclidean distance function between two points in E^3.

Definition 12. DT_2 is a distance function between a point p and a finite set of points S defined as follows:

$$\text{DT}_2(p,S) = \min_{q \in S} \text{DT}_1(p,q).$$

Definition 13. The center of gravity $(\bar{x},\bar{y},\bar{z})$ of a finite set of points $S=\{(x_i,y_i,z_i) \mid i=0,\ldots,n\}$ is defined as follows:

$$\bar{x} = \frac{\sum_{i=0}^{n} x_i}{|S|}, \quad \bar{y} = \frac{\sum_{i=0}^{n} y_i}{|S|}, \quad \bar{z} = \frac{\sum_{i=0}^{n} z_i}{|S|},$$

where $|S|$ denotes the number of points in S.

Definition 14. A position normalized set norm(S) is derived from a finite set of points S as follows:

$$\text{norm}(S) = \{(x_i-\bar{x}, y_i-\bar{y}, z_i-\bar{z}) \mid (x_i,y_i,z_i) \in S\}$$

where $(\bar{x},\bar{y},\bar{z})$ is the center of gravity of S.

Definition 15. DT_3 is a distance function between two finite sets of points S_1 and S_2 defined as follows:

$$\text{DT}_3(S_1,S_2) = \frac{\sum_{p \in \text{norm}(S_1)} \text{DT}_2(p, \text{norm}(S_2))}{|S_1|} + \frac{\sum_{p \in \text{norm}(S_2)} \text{DT}_2(p, \text{norm}(S_1))}{|S_2|}.$$

5.1. Shape distortion under noise

To find shape distortion by a thinning algorithm under pseudo-random contour noise we add random noise on a 3D digital object according to the model presented in Section 3.4 and then estimate the shape distortion in the skeleton. Let $\text{Sk}(X)$ denote the skeleton of a 3D object X. Let $\ddot{X}$ denote the noisy version of X. To find the distortion of shape in the skeleton under noise we compute $\text{DT}_3(\text{Sk}(X), \text{Sk}(\ddot{X}))$. A comparative study between the percentage of noise in $\ddot{X}$ and $\text{DT}_3(\text{Sk}(X), \text{Sk}(\ddot{X}))$ gives a quantitative sense about the robustness of a thinning algorithm under noise. A comparative study on the objects of Figs 11,12 and 13, under different amount of noise, is shown in Fig. 14.

5.2. Shape distortion under rotation

Here, we study the shape distortion by the thinning algorithm under rotation. Let $[X]_{\theta,\omega,\psi}$ denote the 3D digital object obtained from a 3D digital object X by a rotation, where θ, ω, ψ determines the new system of axes with the center of gravity of X as the origin. Let $\text{Sk}(X)_{\theta,\omega,\psi}$ denote the rotated form of $\text{Sk}(X)$, where θ, ω, ψ determines the new system of axes with the center of gravity of $\text{Sk}(X)$ as the origin. It is worthy to mention that $[X]_{\theta,\omega,\psi}$ is a rotation in digital space while $\text{Sk}(X)_{\theta,\omega,\psi}$ is a rotation in the Euclidean space. To estimate the shape distortion under rotation we compute $\text{DT}_3(\text{Sk}(X)_{\theta,\omega,\psi}, \text{Sk}([X]_{\theta,\omega,\psi}))$. An experimental study of shape distortion on the objects of Figs 11,12 and 13, under different rotation about the x-, y- and z-axes, are shown in Figs 15–17, respectively.

6. DISCUSSION AND CONCLUSION

A new parallel thinning algorithm of 3D digital images with topology and shape preserving properties has been

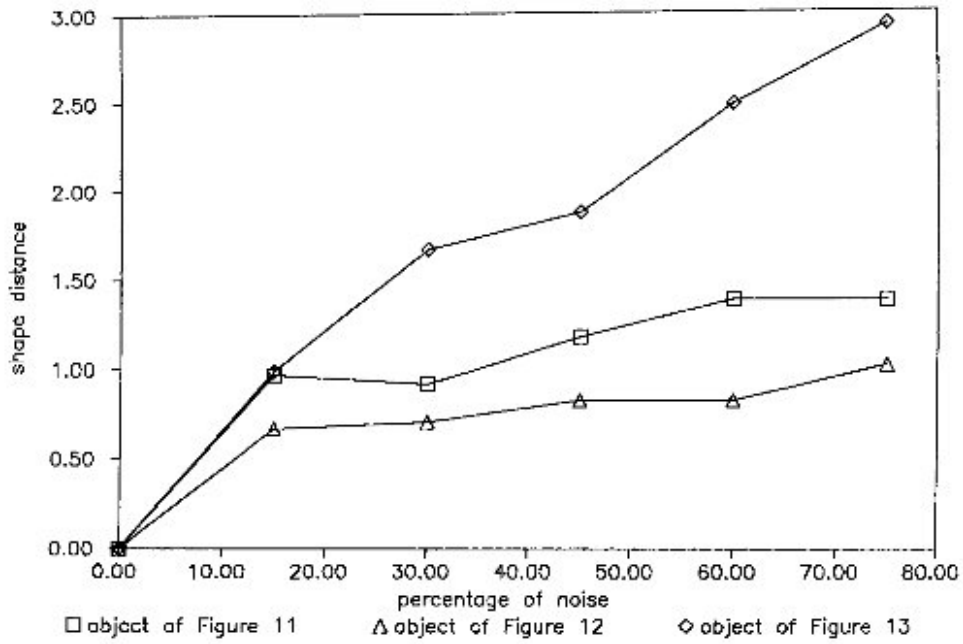

Fig. 14. Shape distortion analysis under pseudo random contour noise for the objects of Figs 11,12 and 13.

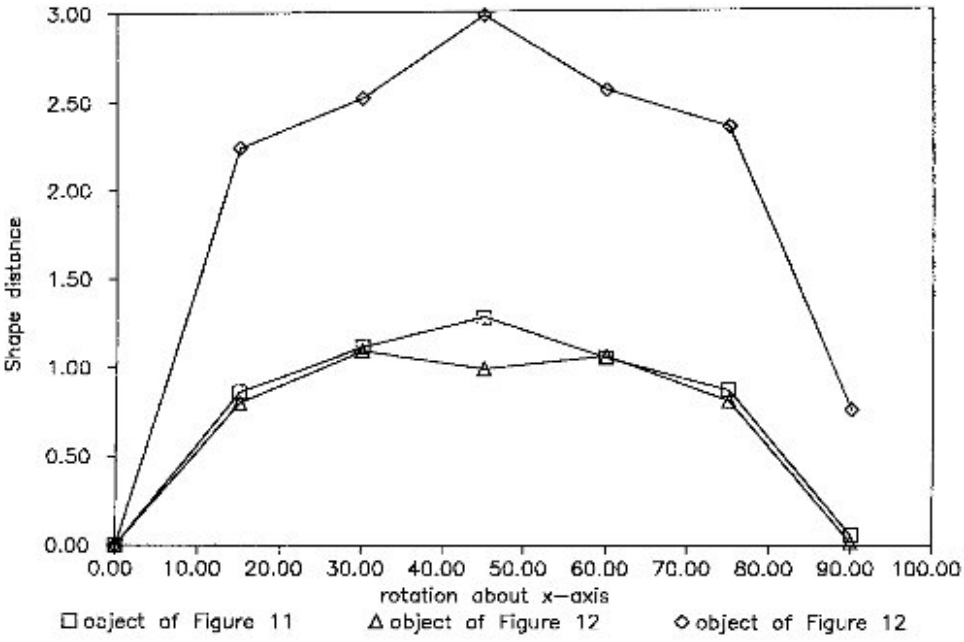

Fig. 15. Shape distortion analysis under rotation about the x-axis for the objects of Figs 11,12 and 13.

developed in this paper. To preserve topology we have applied the concept of simple points.[8–10] On the other hand, the concept of sub-fields[16] has been used for parallel implementation. The concepts of open points and shape points have been introduced and applied to 3D thinning. The role of open points in producing proper skeleton around different types of corners has been justified. Also, the shape points are justified to be robust under noise.

In this paper we have used two versions of the image—one before the current iteration while the other being the currently processed image. The necessity of two image versions in parallel thinning has been justified. This concept has made a major improvement in the quality of thinned image. The results of application of the parallel thinning algorithm on several synthetically generated 3D objects and their noisy versions have been presented. We have also described an algorithm that

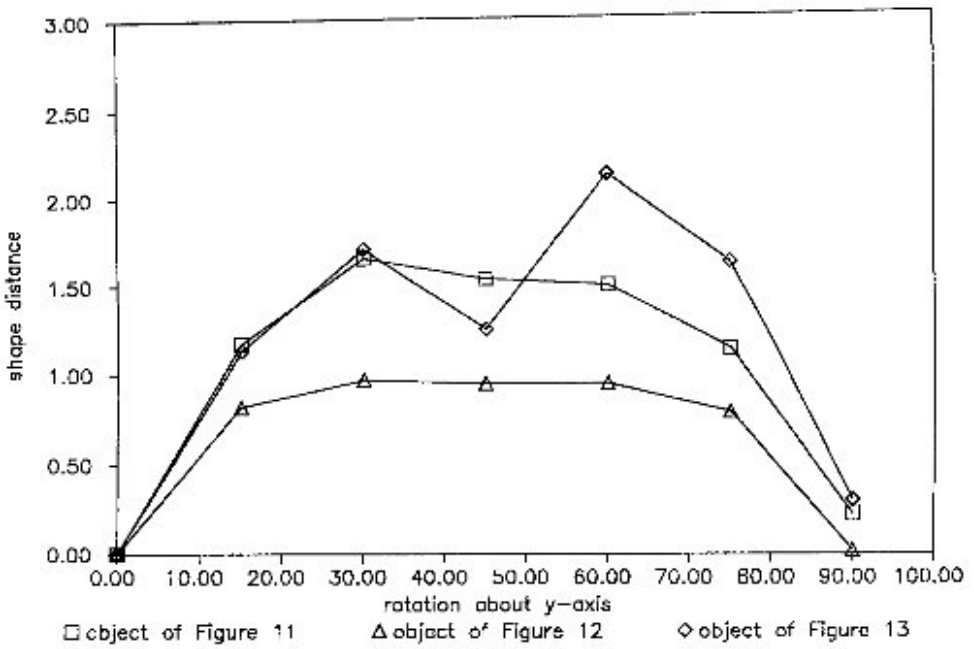

Fig. 16. Shape distortion analysis under rotation about the y-axis for the objects of Figs 11,12 and 13.

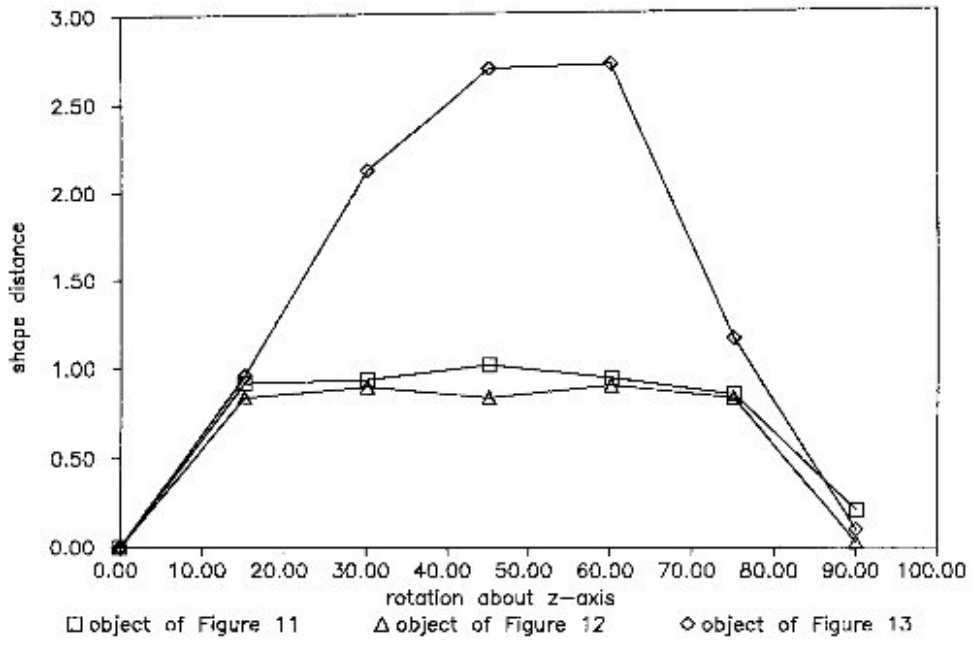

Fig. 17. Shape distortion analysis under rotation about the z-axis for the objects of Figs 11,12 and 13.

produces a medial arc representation of an object from its surface representation.

In the literature of 3D thinning there are enough publications[3,6,8 11,14] where the topology preservation is ensured during thinning. Shape preservation has received less attention, especially in noisy images. In practice, the shape of a skeleton gets distorted under noise and rotation. The distortion, among others, characterizes the goodness of an algorithm. To estimate the degree of distortion we have used the concept of shape distance. The robustness of our algorithm under pseudo-random contour noise and rotation has been studied and presented with examples. Because of digital nature of the image space, a shape may be distorted under rotation which is also reflected in the skeleton. A part of the skeletal distortion shown in Figs 15,16 and 17 is because of this reason. It is understood from Figs 15,16 and 17 that shape distortion is maximum for a rotation around

45°, which is quite expected. Also, for this thinning algorithm the shape distortion increases more or less linearly with the percentage of noise.

Acknowledgements—We are thankful to the unnamed referee for his/her constructive comments which helped us to improve this paper.

REFERENCES

1. P. K. Saha and B. B. Chaudhuri, 3D Digital topology under binary transformation with applications, *CVGIP: Image Understanding* **63**(3), 418–429 (1996).
2. S. N. Srihari, J. K. Udupa and M. Yau, Understanding the bin of parts, in *Proc. Int. Conf. on Cybernetics and Society*, Denver, Colorado, pp. 44–49 (1979).
3. C. M. Ma, On topology preservation in 3D thinning, *CVGIP: Image Understanding* **59**, 328–339 (1994).
4. K. J. Hafford and K. Preston, Jr Three-dimensional skeletonization of elongated solids, *Comput. Vision Graphics Image Process.* **27**, 78–91 (1984).
5. S. Lobregt, P. W. Verbeek and F. C. A. Groen, Three-dimensional skeletonization: Principle and algorithm, *IEEE Trans. Pattern Analysis Mach. Intell.* **PAMI-2**, 75–77 (1980).
6. D. G. Morgenthaler, Three-dimensional simple points: Serial erosion, parallel thinning and skeletonization, Technical Report TR-1005, Computer Vision Laboratory, University of Maryland (1981).
7. J. Mukherjee, P. P. Das and B. N. Chatterjee, Thinning of 3-D images using the safe point thinning algorithm (SPTA), *Pattern Recognition Lett.* **10**, 167–173 (1989).
8. P. K. Saha, B. Chanda and D. Dutta Majumder, Principles and algorithms for 2D and 3D shrinking, Technical Report TR/KBCS/2/91, N.C.K.B.C.S. Library, Indian Statistical Institute, Calcutta, India (1991).
9. P. K. Saha, B. B. Chaudhuri, B. Chanda and D. D. Majumder, Topology preservation in 3D digital space, *Pattern Recognition* **27**(2), 295–300 (1994).
10. P. K. Saha and B. B. Chaudhuri, Detection of 3-D simple points for topology preserving transformations with application to thinning, *IEEE Trans. Pattern Analysis Mach. Intell.* **16**(10), 1028–1032 (1994).
11. P. K. Saha and B. B. Chaudhuri, Simple point computation and 3-D thinning with parallel implementation, Technical Report TR/KBCS/1/93, N.C.K.B.C.S. Library, Indian Statistical Institute, Calcutta, India (1993).
12. S. N. Srihari, Representation of three-dimensional digital images, *ACM Comput. Surveys* **13**, 399–424 (1981).
13. J. I. Toriwaki, S. Yokoi, T. Yonekura and T. Fukumura, Topological properties and topology-preserving transformation of a three-dimensional binary picture, in *Proc. Sixth Int. Conf. on Pattern Recognition*, pp. 414–419 (1982).
14. Y. F. Tsao and K. S. Fu, A parallel thinning algorithm for 3D pictures, *Comput. Graphics Image Process.* **17**, 315–331 (1981).
15. Y. F. Tsao and K. S. Fu, A 3D parallel skeletonwise thinning algorithm, in *Proc. IEEE PRIP Conf.*, pp. 678–683 (1982).
16. M. J. E. Golay, Hexagonal parallel pattern transformations, *IEEE Trans. Comput.* **C-18**, 733–740 (1969).
17. N. J. Naccache and R. Shingal, SPTA: A proposed algorithm for thinning binary patterns, *IEEE Trans. Systems Man Cybernet.* **SMC-14**, 409–418 (1984).
18. C. M. Ma, Topology preservation on 3D images, in *Proc. SPIE Conf. on Vision Geometry*, Boston, Massachusetts (1993).
19. L. Zusne, *Visual Perception of Forms*. Academic Press, New York (1970).
20. F. Attneave, *Application of Information Theory to Psychology*. Holt, New York (1959).
21. T. Y. Kong and A. Rosenfeld, Digital topology: Introduction and survey, *Comput. Vision Graphics Image Process* **48**, 357–393 (1989).
22. P. K. Saha and B. B. Chaudhuri, A new approach of computing Euler characteristic, *Pattern Recognition* **28**(12), 1955–1963 (1995).
23. D. K. Banerjee, S. K. Parui and D. D. Majumder, A shape metric for 3D objects, *Indian J. Pure Appl. Math.* **25**(1\2), 95–11_ (January\February 1994).
24. D. Dutta Majumder, The Indian KBCS/FGCS programme and some applications of pattern recognition and computer vision, *IE(I) J. CP* **74** (November 1993).

About the Author—PUNAM KUMAR SAHA obtained his Bachelors and Masters degree in Computer Science and Engineering from Jadavpur University in 1987 and 1989 respectively. He joined Electronics and Computer Sciences Unit, Indian Statistical Institute, as a Senior Research Fellow in 1989 where he is presently working as a faculty member. His area of research interest includes three-dimensional digital topology and its applications to image processing and computer vision, fractal geometry and scale space analysis. He has communicated/published several papers in reputed journals. He has received *Young Scientist* award from the Indian Science Congress Association for best Computer Science oriented work "A New Thinning and Segmentation Approach for 3D Digital Images" in 1996. He is a member of International Association of Pattern Recognition (IAPR).

About the Author—B. B. CHAUDHURI received his B.Sc. (Hons), B.Tech. and M.Tech. degrees from Calcutta University, India, in 1969, 1972 and 1974, respectively and Ph.D. degree from Indian Institute of Technology, Kanpur, in 1980. He joined Indian Statistical Institute in 1978 where he served as the Project Co-ordinator and Head of National Nodal Center for Knowledge Based Computing. Currently, he is the head of Computer Vision and Pattern Recognition Unit of the institute. His research interests include Pattern Recognition, Image Processing, Computer Vision, Natural Language Processing and Digital Document Processing including OCR. He has published more than 150 research papers in reputed International Journals and has authored a book entitled *Two Tone Image Processing and Recognition* (Wiley Eastern, 1993). He was awarded *Sir J. C. Bose Memorial Award* for best Engineering Science oriented paper published in *JIETE* in 1986 and *M. N. Saha Memorial Award* (twice) for best application oriented research published in 1989 and 1991. In 1992, he won the prestigious *Homi Bhabha Fellowship* for working on OCR of the Indian Languages and computer communication for the blind. He has been selected for the *Hari Om Ashram Prerit Dr Vikram Sarabhai Research Award* for the year 1995 for his achievements in the fields of Electronics, Informatics and Telematics. Also, he received *C. Achuta Menon Prize* in 1996 for his work on computational linguistics and natural language processing. As a Leverhulme Visiting Fellow, he worked at Queen's University, U.K. Also, he worked as a Visiting Faculty Member at GSF, Munich, and Guest Scientist at the Technical University of

Hannover during 1986–88 and again in 1990–91. He is a Senior member of IEEE, member secretary (Indian section) of International Academy of Sciences, Fellow of National Academy of Sciences (India), Fellow of the Indian National Academy of Engineering. He is serving as a Associate Editor of the journals *Pattern Recognition* and *Vivek* as well as Guest Editor of a special issue of *Journal IETE* on Fuzzy Systems.

About the Author – DWIJESH DUTTA MAJUMDER obtained his M.Sc. (Tech.) degree in Radio Physics and Electronics and Ph.D. in Digital Computers' Memory Technology in 1955 and 1962, respectively, from Calcutta University. Since 1955, he has been working in Indian Statistical Institute in different capacities and was Professor and Head of Electronics and Communication Sciences Unit for 20 years. In 1992, Professor Dutta Majumder was made Professor Emeritus of ISI, Emeritus Scientist of CSIR. He is the author of more than 400 research papers in international journals and conference proceedings and is the author/editor of six books all published by John Wiley and Sons in the areas of memory technology, pattern recognition, man-machine communication, image processing, computer vision, artificial intelligence, expert systems, cybernetics systems theory, data communication, neural modeling and fuzzy mathematics. Professor Dutta Majumder visited and delivered series of lectures on his work in some of the above mentioned subjects in large number of Universities and Industrial Labs in U.S.A., U.K., Japan and Europe as a Guest Professor several times. He is a member of the editorial boards of Pattern Recognition Letters (PRL), Image Processing and Communications (IPC), Indian Journal of Pure and Applied Mathematics (IJPAM), The Journal of Fuzzy Mathematics and is the consulting editor of the Journal of Computer Division of the Institution of Engineers (India). Professor Dutta Majumder is a Fellow of International Association of Pattern Recognition, Indian National Science Academy, Indian National Academy of Engineering, The National Academy of Sciences, Computer Society of India and Institution of Electronics and Telecommunication Engineers, and is a member of the governing Board of IAPR, Director of the World Organisation of Cybernetics and Systems, Presidents of Indian Society of Fuzzy Mathematics and Information Processing (ISFUMIP) and Indian Association for Pattern Recognition and Artificial Intelligence (IAPRAI). He is recipient of Sir J. C. Bose Award of IETE, Sir C. V. Raman Award of ASI, Norbert Wiener Award of WOSC, R. L. Wadhwa Gold Medal of IETE, P. C. Mahalanobis Gold Medal of INSA and several other honors and awards.